Electrochemical liquid-liquid interface between oil and ionic liquid for reductive deposition of metal nanostructures

Yohei Kuroyama, Naoya Nishi,* and Tetsuo Sakka
Department of Energy and Hydrocarbon Chemistry, Graduate School of Engineering, Kyoto University, Kyoto, 615-8510, Japan
nishi.naoya.7e@kyoto-u.ac.jp

Abstract

An electrochemical system at the ionic liquid (IL) | oil (O) interface has been constructed and utilized as electrochemical reaction field for reductive deposition of metal nanostructures. The interface between 1-(3-hydroxypropyl)-3-methyl-imidazolium chloride (C_{3OH}mimCl), a hydrophilic IL, and 1,6-dichlorohexane (containing an organic electrolyte) exhibits a polarized potential window of 150 mV, which is limited by the ion transfer (IT) of the IL cation and anion at the positive and negative edges, respectively. The polarizable IL | O interface has allowed to record voltammograms for the electron transfer (ET) and IT processes across the IL | O interface that are involved in the reductive deposition of gold at the IL | O interface. The ET between $AuCl_4^-$ in the IL phase and decamethylferrocene in the O phase proceeds without applying external voltage by coupling with the IT of $AuCl_4^-$, spontaneously forming Au nanostructures at the IL | O interface.

KEYWORDS: Liquid-liquid interface; ITIES; Metal nanofibers; Interfacial charge transfer; Electrochemical window

1. Introduction

Ionic liquids (ILs) are salts that are liquid around room temperature, with several characteristics such as ionic conductivity, a wide potential window at the electrode interface, high thermal stability, negligibly low vapor pressure, and flame retardancy [1,2]. These characteristics make ILs peculiar and different from conventional molecular liquids such as water (W) and oil (O) [3,4].

The interface between two immiscible electrolyte solutions (ITIES) is known to be an electrochemical reaction field. For example, metal nanoparticles are formed at the W | O interface by electron transfer (ET) between a metal precursor dissolved in one phase (mainly W) and a reducing agent in the other phase [5–9] by using electrochemistry at the polarizable W | IL interface [10–15] . The same methodology can be realized at the W | IL interface for the formation of metal nanostructures [16–27]. Our group found that the reduction of Au [23–25], Pt [26], Pd [27], and Ag [18] at the IL | W interface produces unique metal 1D nanostructures such as dendritic nanofibers [23,24,26], nanofiber arrays [27], and nanobelts [18], due to the interfacial structure ordering [28–30] and high viscosity [19,23] of ILs.

The successful applications of this liquid-liquid interfacial method at the IL | W interface motivated us to explore another liquid-liquid interface, which is the IL | O interface. The IL | O interface is intriguing because it is regarded as a water-free reaction field and can be applied to reactions in which products and reactants are water-reactive. One pioneering study by Cousens and Kucernak found that the IL | O interface can be polarizable by using ethylammonium nitrate (EAN) as the hydrophilic IL and 1,6-dibromohexane (DBH) or a cyclohexane/1,2-

dichloroethane mixture (O_{mix}) as the O [31]. However, to the best of our knowledge, there are no reports on the measurements of ET and ion transfer (IT) across the IL | O interface, as well as the formation of metal nanostructures at the IL | O interface. The IL | O interface has not been explored in the electrochemistry of ITIES.

In the present study, we present a new electrochemical system at the IL | O interface using a hydrophilic Cl^--based IL where the IT and ET processes can be measured electrochemically. Cl^--based ILs are beneficial for the reductive deposition of metals, because excess Cl^- in the ILs stabilizes chloride complexes such as $AuCl_4^-$ and $PtCl_4^{2-}$ used as metal precursors [5,6,8,16,17,23–27]. We report that the formation of metal nanostructures is possible at the IL | O interface, exemplified by Au, which has been accomplished at the W | O [5,32–43] and W | IL [16,17,22–25] interfaces. Electrochemistry measurements clearly illustrate that the reductive deposition of Au can spontaneously occur via ET at the IL | O interface between $AuCl_4^-$ in the IL phase and a reductant in the O phase by coupling with IT of $AuCl_4^-$.

2. Experimental

2.1 Reagent

To realize the polarizable IL | O interface, the hydrophilicity of IL ions is a key parameter. This is just an opposite case with the IL | W interface where the hydrophobic IL ions lead to wide potential window (PW) [10,11,44]. To choose a cation that is combined with Cl^-, we took into account not only the ionic hydrophilicity but also the melting point of the salt, which are in the trade-off relationship. Among Cl^--based ILs, 1-(3-hydroxypropyl)-3-methylimidazolium chloride (C_{3OH}mimCl), which is a room temperature IL, was chosen as a hydrophilic IL for the IL-O two-phase system, because $C_{3OH}mim^+$ is relatively hydrophilic (see Table 1 for ionic hydrophilicity and melting points of several ILs). C_{3OH}mimCl was synthesized using 1-chloropropanol and 1-methylimidazole (both from TCI), according to a reported method [45]. $AuCl_3$ (Shimadzu) was added into C_{3OH}mimCl to form $AuCl_4^-$ in the IL [46]. The IL solution was stirred at 50 °C for about 6 hours and then residual H_2O in the IL was removed by an oil pomp. 1,6-dichlorohexane (DCH, TCI), and dichloromethane (DCM, Kishida Chemical) were used as O. Decamethylferrocene (DMFc, Wako) was used as a reducing agent. The water contents of C_{3OH}mimCl, DCH, and DCM determined by the Karl Fischer coulometer (CA-21, Mitsubishi Chemical) are 13000, 280, and 120, respectively. For electrochemical measurements, tetraoctylammonium tetraphenylborate (TOATPB, synthesized from tetraoctylammonium bromide and sodium tetraphenylborate by metathesis reaction) was added to O as a supporting electrolyte.

Table 1. Characteristics of hydrophilic ILs.

IL	Melting point (°C)	$\Delta_O^W\phi_C^0$ [a] (V)	$\Delta_O^W\phi_A^0$ [b] (V)	$\Delta_O^W\varphi_C^0 - \Delta_O^W\varphi_A^0$ [c] (V)	PW (V)
C_{3OH}mimCl	＜25	+0.06 [d]	-0.53 [h]	0.59	0.15 [i]
C_2mimCl	84	-0.03 [e]	-0.53 [h]	0.50	
C_{2OH}mimCl	83	+0.09 [f]	-0.53 [h]	0.64	
EAN	12	+0.17 [g]	-0.35 [h]	0.52	0.10 [j] 0.15 [k]

a : The standard ion-transfer potential at the W | O interface for an IL cation.
b : The standard ion-transfer potential at the W | O interface for an IL anion.
c : A measure of PW [47].
d : Estimated from $\Delta_O^W\varphi_i^0$ for $C_{2OH}mim^+$ with the methylene contribution to log*P* (O = 1-octanol (OcOH)) in alkanes [25].
e : Ref. [48] (O = nitrobenzene).
f : Estimated from $\Delta_O^W\varphi_i^0$ for C_2mim^+ with the log*P* (O = OcOH) difference between alkanes and alkahols [25].
g : Extrapolated from the chain length dependence of $\Delta_O^W\varphi_i^0$ for alkylammonium (O =NB, unpublished data).
h : Ref. [49] (O = DCE).
i : Present study at the IL | DCH interface.
j : At the IL | DBH interface [31].
k : At the IL | O_{mix} interface [31].

2.2 Electrochemical measurement

2.2.1 CV for PW or IT measurements

Electrochemical measurements at the IL | O interface (O = DCH) were performed using a micropipette to minimize the effect of ohmic drops in the IL and O bulk. The PW and IT were measured at the micro liquid-liquid interface formed at the tip of the micropipette [50,51]. A micropipette with a tip inner diameter of 10 μm was filled with IL and was immersed in O to form micro IL | O interface at

the tip of the micropipette. The two-electrode electrochemical cell is represented as below,

Ag/AgCl	10 mM LiCl 10 mM NaTPB (W_{ref})	10 mM TOATPB (O)	C_{3OH}mimCl *x* $AuCl_4^-$ (IL)	Ag/AgCl

(Cell I)

where x is the mole fraction of $AuCl_4^-$ in the IL ($n_{AuCl_4^-}/(n_{Cl^-} + n_{AuCl_4^-})$; n_i is the molar amount of species i). We set to $x = 0$ for PW measurement and $x = 0.01$ for the measurement of IT of $AuCl_4^-$. A glass cylinder with an inner diameter of 0.6 mm filled with W_{ref} was also immersed in O as a reference electrode for the O side. Ag/AgCl wires were inserted into the micropipette and glass cylinder. A potentiostat (HECS 972, Huso Electro Chemical System) was used for the measurement. The potential of Ag/AgCl on the right side with respect to the left side in the cell equation is denoted as E. The current I due to the transfer of cations (anions and electron) from IL to O (from O to IL) is taken to be positive.

2.2.2 CV for ET measurement

In order to measure only ET without ITs, metals were inserted between the IL and O phases (see Fig. S1 for the schematic) as was proposed in the ET measurement at the W | O interface [52]. The electrochemical cell is as follows.

Ag/AgCl	10 mM LiCl 10 mM NaTPB (W_{ref})	10 mM TOATPB (O)	Pt	Au	C_{3OH}mimCl x $AuCl_4^-$ (IL)	Ag/AgCl

(Cell II)

Au wire was immersed in IL filled in a sample tube, and a Pt microelectrode having a tip diameter of 10 μm was immersed in O. The Au wire and the Pt microelectrode were electrically connected by a conductive wire. The other conditions are the same as those in 2.2.1.

2.3 Reductive deposition of Au at the IL | O interface

The IL-O two-phase system was constructed using $AuCl_4^-$ (x = 0.01) containing IL and 18 mM DMFc containing DCH or DCM as O without applying the external potential. After being kept for 3 days at room temperature, black deposits were obtained at the IL | O interface. After washing with nitrobenzene and methanol, the deposits were observed by SEM (SU 8200, Hitachi High Technologies) and EDX (EMAXEvolution X-Max (detection element area 80 mm^2)). The dissolved species in both phases before and after reactions were confirmed by UV-vis measurement ((UV-1900i, Shimadzu).

3. Results and discussion

3.1 Electrochemical measurement

3.1.1 CV for PW or IT measurements

The CVs of PW and IT measurements are shown in Fig. 1a and b, respectively. The PW with 150 mV at the C_{3OH}mimCl | DCH interface was obtained (Fig. 1a). This is wider than EAN | DBH (100 mV) and similar to the EAN | O_{mix} interface (150 mV) reported by Cousens and Kucernak [31]. On the other hand, it is significantly narrower than the PW at the W | DCH interface (800 mV) measured by Katano and Senda [53], because of the fact that C_{3OH}mimCl is less hydrophilic (lipophobic) than W. The negative edge of PW is likely to be limited by IT of Cl^- (IL → O), not by TOA^+ (O → IL), judging from more positive standard potential

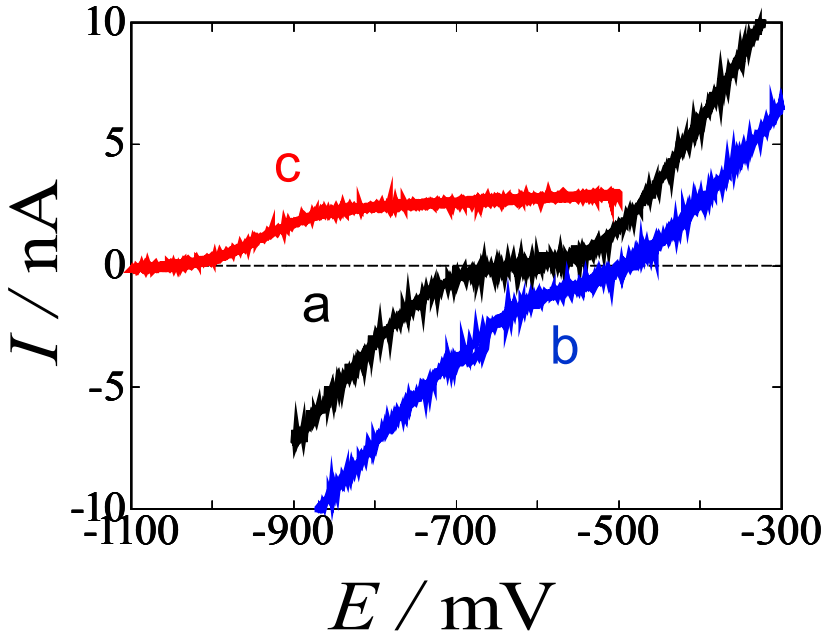

Fig. 1. CVs at the C_{3OH}mimCl (IL) | DCH (O) interface for (a) PW, (Cell I) (b) IT (transfer of $AuCl_4^-$, Cell I), and (c) ET (Cell II) measurements. Scan rate: 20 mV s^{-1}.

for Cl^- (–0.53 V at the W | DCE interface [49]) than TOA^+ (–0.75 V at the W | DCE interface estimated from the extrapolation of the chain length dependence for tetraalkyl ammonium [49,54–56] (Fig. S2)). On the other hand, the PW positive edge is limited by either of IT of $C_{3OH}mim^+$ (IL → O) or TPB^- (O → IL). As a control experiment the CVs at the W | O interface were recorded, where neat $C_{3OH}mimCl$ was replaced with 10 mM LiCl aqueous solution without and with 1 mM $C_{3OH}mimCl$ for the PW and IT measurements, respectively. The CVs are shown in Fig. S3. The PW CV (black) in Fig. S3 exhibits PW of 800 mV in agreement with the result by Katano and Senda [53]. In the IT CV (red), one can see currents around –100 mV, which is ascribable to IT of $C_{3OH}mim^+$. The fact that IT of $C_{3OH}mim^+$ (W → O) was observed within the PW indicates that the standard ion transfer potential of $C_{3OH}mim^+$ is more negative than that of TPB^-. Therefore, the positive edge of the PW at the IL | O interface is likely to be limited by the IT of $C_{3OH}mim^+$ (IL → O).

The CV for IT in Fig. 1b shows a negative current over the PW compared to the PW CV in Fig. 1a. This negative current is ascribable to IT of $AuCl_4^-$ (IL → O).

$$AuCl_4^- \text{ (IL)} \rightarrow AuCl_4^- \text{ (O)} \quad (1)$$

The standard potential for IT of $AuCl_4^-$ is located around the positive edge of PW which is limited by $C_{3OH}mim^+$. This is reasonable because the standard potential for IT of $AuCl_4^-$ (+0.115 V [57]) across the W | DCE interface is more positive than that of $C_{3OH}mim^+$ (+0.06 V, Table 1).

187

188 3.1.2 CV for ET measurement

189 Fig. 1c shows the CV of ET at the IL | O interface. The positive current starts to
190 flow from potential more negative than the potential window due to ET of e^- (O
191 → IL).

192

$$AuCl_4^- \text{ (IL)} + 3DMFc \text{ (O)} \rightarrow Au + 3DMFc^+ \text{ (O)} + 4Cl^- \text{ (IL)} \quad (2)$$

193

194 Fig. 1b and 1c show a negative current due to IT and a positive current due to ET
195 within the PW, respectively. Thus, the coupling of IT and ET [58] within the PW
196 should result in spontaneous redox reactions while keeping electrical neutrality.
197 The net reaction for the coupled ET and IT is:

198

$$\begin{aligned} &3AuCl_4^- \text{ (IL)} + 3DMFc \text{ (O)} \\ &\rightarrow Au + 3DMFc^+ \text{ (O)} + 4Cl^- \text{ (IL)} + 3AuCl_4^- \text{ (O)}. \end{aligned} \quad (3)$$

199

200 The standard Gibbs energy ΔG^0 for Eq. (3) can be estimated from the CVs shown
201 in Fig. 1 where the standard potentials of ET ($AuCl_4$-DMFc) and IT ($AuCl_4^-$) are
202 estimated to be –0.95 V and –0.55 V, respectively. The potential difference, –0.40
203 V, corresponds to $\Delta G^0 = -120$ kJ/mol.

204

205 3.2 Reductive deposition of Au using the IL | O interface as a reaction field

206 3.2.1 Appearance of deposited Au

Fig. 2 shows the SEM images of deposited Au obtained at the IL | O interface using DCM or DCH as O. The deposits were confirmed to be metalic Au by EDX. When DCH was used as O, the deposited Au was microsized spherical. When DCM was used as O, the deposited Au was needle-like in nano size, with dendritic structures. This morphology difference may result from the viscosity of DCH and DCM. One-dimensional Au nanostructures were obtained at the IL | W interface where the IL viscosity is three orders of magnitude greater than W [19,23]. In the present study, the viscosity difference between C_{3OH}mimCl (2000 mPa s at 25 ℃ [30]) and DCM (0.40 mPa s at 25 ℃ [60]) was similar to the previous cases. Even for the DCH (2.04 mPa s at 25 ℃ [61]) case the viscosity difference is huge but the obtained Au structure was not one-dimensional. These results suggest that the viscosity difference is not the only factor to induce one-dimensional nanostructure formation. Other factors include the interfacial structure of ILs as was found in our previous study [19]. Furthermore, to investigate the effect of water content in IL on the Au morphology, a control experiment was carried out in which 1 M HCl aqueous solution was added to IL at 10 wt%. Fig. S4 shows an SEM image of the Au deposit. The structure is basically similar to that without the addition of the HCl solution (Fig. 2a), although the tip part is shorter, which seems to result from the decrease in viscosity due to the addition of water.

226

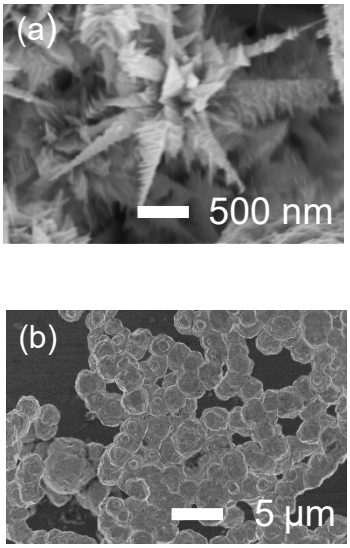

Fig. 2 SEM images of Au deposited at (a) the C_{3OH}mimCl｜DCM and (b) the C_{3OH}mimCl｜DCH interfaces.

227

228

229 ### 3.2.2 Reaction Mechanism of Au Reduction at the IL | O Interface

230 The photographs of the IL-O two-phases system (O = DCM) before and during
231 the reaction are shown in Fig. 3. Fig. 3a shows O solution of DMFc before the
232 reaction whose color is yellow due to DMFc. Onto the O solution we added IL

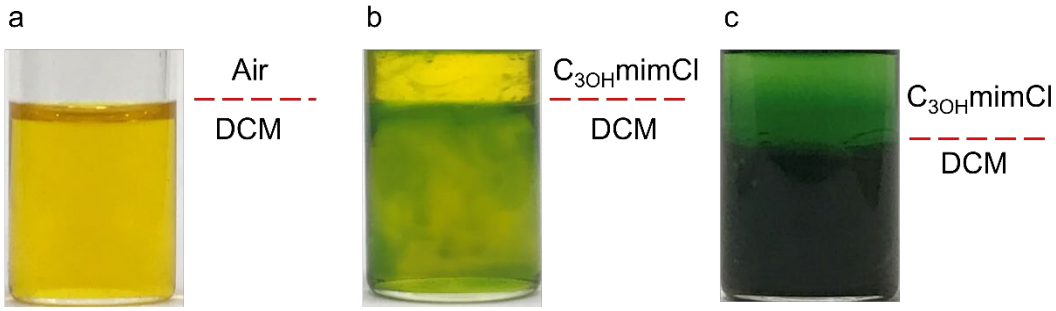

Fig. 3. Photographs for the reaction process at the C_{3OH}mimCl ($AuCl_4^-$) | DCM (DMFc) interface (a) before, (b) immediately after, and (c) three days after the addition of the upper C_{3OH}mimCl phase.

233 containing $AuCl_4^-$, which is also yellow due to $AuCl_4^-$. Fig. 3b shows the system
234 just after the two-phase formation. The O side of the IL | O interface immediately
235 changed to green. This is because DMFc is oxidized to $DMFc^+$ via the ET (Eq. 2).
236 Over time, the green color diffused to the O bulk and became denser as shown is
237 Fig. 3c that is for after 3 days. One can notice in Fig. 3c that the IL phase also
238 became greenish, although the color is much paler. This means that a small fraction
239 of $DMFc^+$ has transferred from O to IL.

240

$$DMFc^+ (O) \rightarrow DMFc^+ (IL) \quad (3)$$

241

The $DMFc^+$ in each phase after reaction was determined using UV-vis measurements. Fig. S5 shows the UV-vis spectra for O (black) and IL (red) both of which were diluted with methanol. $DMFc^+$ absorption peak appears at 780 nm. The molar amount of $DMFc^+$ in each phase was compared by examining the absorbance. The $DMFc^+$ present in the IL phase is 16 times lower than that in the O phase. Therefore, most (94 %) of the generated $DMFc^+$ by the reaction remains in the O phase, and a small fraction (6 %) of $DMFc^+$ transfers to the IL phase.

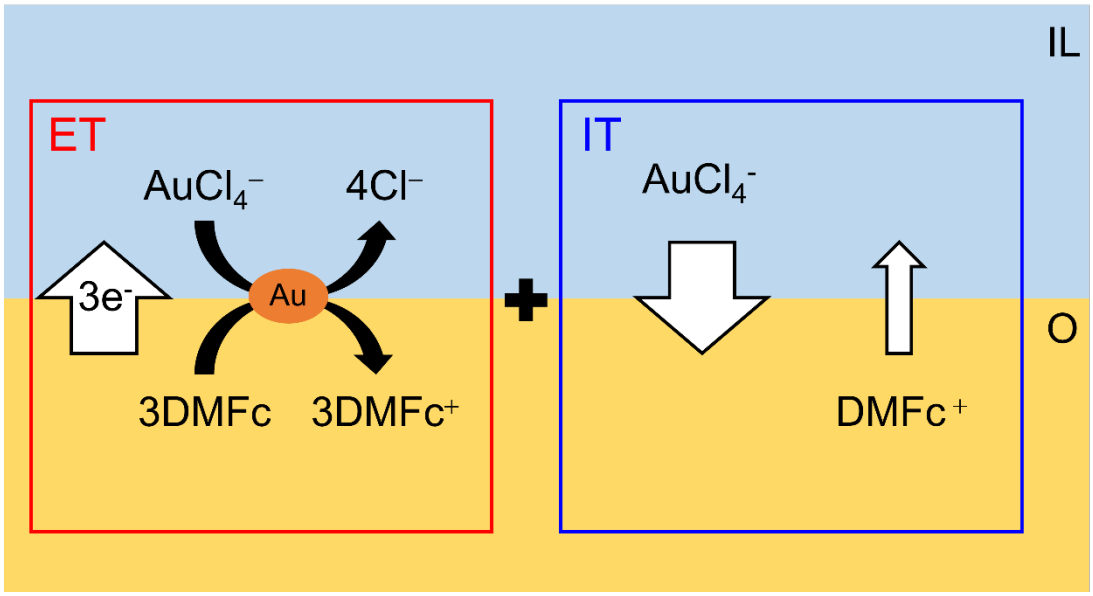

Fig. 4. Reduction deposition mechanism of Au at the IL | O interface.

Based on the above results, we propose the mechanism of reductive deposition of gold as shown in Fig. 4. The reduction of Au (Eq. 2) at the IL | O interface which is ET of e^- (O → IL) releases the hydrophilic Cl^- into the IL phase and the hydrophobic $DMFc^+$ into the O phase. At the same time, IT with a small amount of $DMFc^+$ (O → IL) occurs and partly counters the electrical unbalance of the two phases caused by ET. This is indicated by the slight color change of the IL phase

to green, although it is much less than that of the O phase (Fig. 3c). If all of the generated $DMFc^+$ ions had been transferred to the IL phase, the electric neutrality condition would be maintained by Eqs. 2 and 3. However, as the reaction proceeds, the O phase remains densely green and the quantitative comparison using the UV-vis spectra (Fig. S5) indicates that 94 % $DMFc^+$ remains in the O phase. Therefore, IT of another ion should occur to keep the electrical neutrality. In the present case, it is IT of $AuCl_4^-$ (IL → O) which was confirmed to occur at potential much more positive than IT of Cl^- (IL → O) from the above electrochemical measurement (Fig. 2a). Our previous studies at the IL | W interface also show that IT of $AuCl_4^-$ from W to IL is coupled with ET for the Au deposition [23–25]. With the information altogether, the reaction occurred by the coupling of e^- (O → IL) ET with two ITs, mainly $AuCl_4^-$ (IL → O) and $DMFc^+$ (O → IL) with a small degree.

4. Conclusions

An electrochemical system at the IL | O interface was constructed to design a new electrochemical reaction field. A PW of 150 mV was obtained at the C_{3OH}mimCl | DCH interface using C_{3OH}mimCl, a hydrophilic IL composed of Cl^- as a constituent anion. IT and ET across the C_{3OH}mimCl | DCH interface were measured as current, illuminating that the Au deposition reaction occurs spontaneously by the coupling of IT and ET within the PW, so that the electroneutrality is maintained.

The electrochemistry at the IL | O interface is not limited to the reductive deposition of noble metals like gold. This water-free interface can be used in a wide range of applications, such as the fabrication of base metal nanostructures which is impossible at the conventional W | O and W | IL interfaces. Another example could be interfacial polymerization where ions are involved and water should be avoided.

Acknowledgements

This work was partly supported by JSPS KAKENHI (No. 18K05171) and Kato Foundation for Promotion of Science (KJ-2819).

References

[1] X. Wang, M. Salari, D. Jiang, J. Chapman Varela, B. Anasori, D.J. Wesolowski, S. Dai, M.W. Grinstaff, Y. Gogotsi, Electrode material–ionic liquid coupling for electrochemical energy storage, Nat. Rev. Mater. 5 (2020) 787. https://doi.org/10.1038/s41578-020-0218-9.

[2] A. Lahiri, G. Pulletikurthi, F. Endres, A review on the electroless deposition of functional materials in ionic liquids for batteries and catalysis, Front. Chem. 7 (2019) 1–13. https://doi.org/10.3389/fchem.2019.00085.

[3] Y.-L. Wang, B. Li, S. Sarman, F. Mocci, Z.-Y. Lu, J. Yuan, A. Laaksonen, M.D. Fayer, Microstructural and Dynamical Heterogeneities in Ionic Liquids, Chem. Rev. 120 (2020) 5798–5877. https://doi.org/10.1021/acs.chemrev.9b00693.

[4] M. V. Fedorov, A.A. Kornyshev, Ionic Liquids at Electrified Interfaces, Chem. Rev. 114 (2014) 2978–3036. https://doi.org/10.1021/cr400374x.

[5] Y. Cheng, D.J. Schiffrin, Electrodeposition of metallic gold clusters at the water/1,2-dichloroethane interface, J. Chem. Soc. - Faraday Trans. 92 (1996) 3865–3871. https://doi.org/10.1039/ft9969203865.

[6] R.A.W. Dryfe, A. Uehara, S.G. Booth, Metal deposition at the liquid-liquid interface, Chem. Rec. 14 (2014) 1013–1023. https://doi.org/10.1002/tcr.201402027.

[7] C.N.R. Rao, K.P. Kalyanikutty, The liquid-liquid interface as a medium to generate nanocrystalline films of inorganic materials, Acc. Chem. Res. 41 (2008) 489–499. https://doi.org/10.1021/ar700192d.

[8] A. Trojánek, J. Langmaier, Z. Samec, Electrocatalysis of the oxygen reduction at a polarised interface between two immiscible electrolyte solutions by electrochemically generated Pt particles, Electrochem. Commun. 8 (2006) 475–481. https://doi.org/10.1016/j.elecom.2006.01.004.

[9] C. Johans, R. Lahtinen, K. Kontturi, D.J. Schiffrin, Nucleation at liquid|liquid interfaces: Electrodeposition without electrodes, J. Electroanal. Chem. 488 (2000) 99–109. https://doi.org/10.1016/S0022-0728(00)00185-6.

[10] T. Kakiuchi, N. Tsujioka, K. Sueishi, N. Nishi, M. Yamamoto, Polarized Potential Window Available at the Interface Between an Aqueous Electrolyte Solution and Tetraalkylammonium Imide Salts, Electrochemistry. 72 (2004) 833–835. https://doi.org/10.5796/electrochemistry.72.833.

[11] N. Nishi, S. Imakura, T. Kakiuchi, Wide Electrochemical Window at the Interface between Water and a Hydrophobic Room-Temperature Ionic Liquid of Tetrakis[3,5-bis(Trifluoromethyl)phenyl]borate, Anal. Chem. 78 (2006) 2726–2731. https://doi.org/10.1021/ac052152o.

[12] T.J. Stockmann, P.D. Boyle, Z. Ding, Preparation and crystal structure of tetraoctylphosphonium tetrakis(pentafluorophenyl)borate ionic liquid for electrochemistry at its interface with water, Catal. Today. 295 (2017) 89–94. https://doi.org/10.1016/j.cattod.2017.05.030.

[13] T.J. Stockmann, Z. Ding, Tetraoctylphosphonium Tetrakis(pentafluorophenyl)borate Room Temperature Ionic Liquid toward

335 Enhanced Physicochemical Properties for Electrochemistry, J. Phys. Chem.
336 B. 116 (2012) 12826–12834. https://doi.org/10.1021/jp3081832.
337 [14] J. Langmaier, Z. Samec, Cyclic voltammetry of ion transfer across a room
338 temperature ionic liquid membrane supported by a microporous filter,
339 Electrochem. Commun. 9 (2007) 2633–2638.
340 https://doi.org/10.1016/j.elecom.2007.08.014.
341 [15] Y. Wang, T. Kakiuchi, Y. Yasui, M. V. Mirkin, Kinetics of Ion Transfer at
342 the Ionic Liquid/Water Nanointerface, J. Am. Chem. Soc. 132 (2010)
343 16945–16952. https://doi.org/10.1021/ja1066948.
344 [16] I. Kaminska, J. Niedziolka-Jonsson, A. Roguska, M. Opallo,
345 Electrodeposition of gold nanoparticles at a solid|ionic liquid|aqueous
346 electrolyte three-phase junction, Electrochem. Commun. 12 (2010) 1742–
347 1745. https://doi.org/10.1016/j.elecom.2010.10.011.
348 [17] K. Yao, Q. Huang, W. Lu, A. Xu, X. Li, H. Zhang, J. Wang, A facile
349 synthesis of gold micro/nanostructures at the interface of 1,3-
350 dibutylimidazolium bis(trifluoromethylsulfonyl)imide and water, J. Colloid
351 Interface Sci. 480 (2016) 30–38. https://doi.org/10.1016/j.jcis.2016.06.074.
352 [18] Y. Zhang, N. Nishi, T. Sakka, Interface-templated synthesis of single-
353 crystalline silver chain-like nanobelts at the liquid-liquid interface between
354 water and redox-active ionic liquid, Colloids Surfaces A Physicochem.
355 Eng. Asp. 597 (2020) 124747.
356 https://doi.org/10.1016/j.colsurfa.2020.124747.
357 [19] T. Kakinami, N. Nishi, K. Amano, T. Sakka, Preparation of Dendritic Gold
358 Nanofibers Using a Redox Reaction at the Interface between an Ionic

359 Liquid and Water: Correlation between Viscosity and Nanostructure,
360 Bunseki Kagaku. 65 (2016) 157–161.
361 https://doi.org/10.2116/bunsekikagaku.65.157.
362 [20] K. Yao, Z. Li, X. Li, W. Lu, A. Xu, H. Zhang, J. Wang, Tunable Synthesis
363 of Ag Films at the Interface of Ionic Liquids and Water by Changing
364 Cationic Structures of Ionic Liquids, Cryst. Growth Des. 17 (2017) 990–
365 999. https://doi.org/10.1021/acs.cgd.6b01196.
366 [21] Y. Chen, M. Chen, J. Shi, J. Yang, D. Zhang, Fabrication of “clean” nano-
367 structured metal materials on ionic liquid/water interface, Mater. Lett. 132
368 (2014) 153–156. https://doi.org/10.1016/j.matlet.2014.06.052.
369 [22] T. Soejima, N. Kimizuka, Ultrathin gold nanosheets formed by
370 photoreduction at the ionic liquid/water interface, Chem. Lett. 34 (2005)
371 1234–1235. https://doi.org/10.1246/cl.2005.1234.
372 [23] N. Nishi, T. Kakinami, T. Sakka, Dendritic nanofibers of gold formed by
373 the electron transfer at the interface between water and a highly
374 hydrophobic ionic liquid, Chem. Commun. 51 (2015) 13638–13641.
375 https://doi.org/10.1039/c5cc05476a.
376 [24] N. Nishi, I. Yajima, K. Amano, T. Sakka, Janus-Type Gold/Polythiophene
377 Composites Formed via Redox Reaction at the Ionic Liquid|Water
378 Interface, Langmuir. 34 (2018) 2441–2447.
379 https://doi.org/10.1021/acs.langmuir.7b03792.
380 [25] S. Takagi, N. Nishi, T. Sakka, Ionic liquid-in-water emulsion-templated
381 synthesis of gold nanoshells at the liquid-liquid interface between water

and primary ammonium-based ionic liquids, Chem. Lett. 48 (2019) 589–592. https://doi.org/10.1246/cl.190146.

[26] Y. Zhang, N. Nishi, K. Amano, T. Sakka, One-dimensional Pt nanofibers formed by the redox reaction at the ionic liquid|water interface, Electrochim. Acta. 282 (2018) 886–891. https://doi.org/10.1016/j.electacta.2018.06.024.

[27] Y. Zhang, N. Nishi, T. Sakka, Template-Free and Spontaneous Formation of Vertically Aligned Pd Nanofiber Arrays at the Liquid-Liquid Interface between Redox-Active Ionic Liquid and Water, ACS Appl. Mater. Interfaces. 11 (2019) 23731–23740. https://doi.org/10.1021/acsami.9b05255.

[28] S. Katakura, K. Amano, T. Sakka, W. Bu, B. Lin, M.L. Schlossman, N. Nishi, Evolution and Reversible Polarity of Multilayering at the Ionic Liquid/Water Interface, J. Phys. Chem. B. 124 (2020) 6412–6419. https://doi.org/10.1021/acs.jpcb.0c03711.

[29] N. Nishi, T. Yamazawa, T. Sakka, H. Hotta, T. Ikeno, K. Hanaoka, H. Takahashi, How Viscous Is the Solidlike Structure at the Interface of Ionic Liquids? A Study Using Total Internal Reflection Fluorescence Spectroscopy with a Fluorescent Molecular Probe Sensitive to High Viscosity, Langmuir. 36 (2020) 10397–10403. https://doi.org/10.1021/acs.langmuir.0c01528.

[30] N. Nishi, J. Uchiyashiki, Y. Ikeda, S. Katakura, T. Oda, M. Hino, N.L. Yamada, Potential-Dependent Structure of the Ionic Layer at the Electrode Interface of an Ionic Liquid Probed Using Neutron Reflectometry, J. Phys.

406 Chem. C. 123 (2019) 9223–9230.
407 https://doi.org/10.1021/acs.jpcc.9b01151.
408 [31] N.E.A. Cousens, A.R. Kucernak, Electrochemistry of the ionic liquid|oil
409 interface: A new water-free interface between two immiscible electrolyte
410 solutions, Electrochem. Commun. 31 (2013) 63–66.
411 https://doi.org/10.1016/j.elecom.2013.03.002.
412 [32] C.N.R. Rao, G.U. Kulkarni, P.J. Thomas, V.V. Agrawal, P. Saravanan,
413 Films of Metal Nanocrystals Formed at Aqueous−Organic Interfaces †, J.
414 Phys. Chem. B. 107 (2003) 7391–7395. https://doi.org/10.1021/jp0340111.
415 [33] V.V. Agrawal, G.U. Kulkarni, C.N.R. Rao, Surfactant-promoted formation
416 of fractal and dendritic nanostructures of gold and silver at the organic–
417 aqueous interface, J. Colloid Interface Sci. 318 (2008) 501–506.
418 https://doi.org/10.1016/j.jcis.2007.10.013.
419 [34] A. Uehara, S.-Y. Chang, S.G. Booth, S.L.M. Schroeder, J.F.W.
420 Mosselmans, R.A.W. Dryfe, Redox and Ligand Exchange during the
421 Reaction of Tetrachloroaurate with Hexacyanoferrate(II) at a Liquid-
422 Liquid Interface: Voltammetry and X-ray Absorption Fine-Structure
423 Studies, Electrochim. Acta. 190 (2016) 997–1006.
424 https://doi.org/10.1016/j.electacta.2015.12.108.
425 [35] K. Luo, S.L.M. Schroeder, R.A.W. Dryfe, Formation of Gold
426 Nanocrystalline Films at the Liquid/Liquid Interface: Comparison of Direct
427 Interfacial Reaction and Interfacial Assembly, Chem. Mater. 21 (2009)
428 4172–4183. https://doi.org/10.1021/cm900077h.

[36] R. Knake, A.W. Fahmi, S.A.M. Tofail, J. Clohessy, M. Mihov, V.J. Cunnane, Electrochemical Nucleation of Gold Nanoparticles in a Polymer Film at a Liquid−Liquid Interface, Langmuir. 21 (2005) 1001–1008. https://doi.org/10.1021/la048277q.

[37] B. Sefer, R. Gulaboski, V. Mirčeski, Electrochemical deposition of gold at liquid–liquid interfaces studied by thin organic film-modified electrodes, J. Solid State Electrochem. 16 (2012) 2373–2381. https://doi.org/10.1007/s10008-011-1613-3.

[38] I. Kaminska, M. Jonsson-Niedziolka, A. Kaminska, M. Pisarek, R. Hołyst, M. Opallo, J. Niedziolka-Jonsson, Electrodeposition of Well-Adhered Multifarious Au Particles at a Solid|Toluene|Aqueous Electrolyte Three-Phase Junction, J. Phys. Chem. C. 116 (2012) 22476–22485. https://doi.org/10.1021/jp307674k.

[39] X. Zhu, Y. Qiao, X. Zhang, S. Zhang, X. Yin, J. Gu, Y. Chen, Z. Zhu, M. Li, Y. Shao, Fabrication of Metal Nanoelectrodes by Interfacial Reactions, Anal. Chem. 86 (2014) 7001–7008. https://doi.org/10.1021/ac501119z.

[40] S. Dutta, S. Sarkar, C. Ray, A. Roy, R. Sahoo, T. Pal, Mesoporous Gold and Palladium Nanoleaves from Liquid–Liquid Interface: Enhanced Catalytic Activity of the Palladium Analogue toward Hydrazine-Assisted Room-Temperature 4-Nitrophenol Reduction, ACS Appl. Mater. Interfaces. 6 (2014) 9134–9143. https://doi.org/10.1021/am503251r.

[41] S. Sachdev, R. Maugi, J. Woolley, C. Kirk, Z. Zhou, S.D.R. Christie, M. Platt, Synthesis of Gold Nanoparticles Using the Interface of an Emulsion

Droplet, Langmuir. 33 (2017) 5464–5472. https://doi.org/10.1021/acs.langmuir.7b00564.

[42] S. Sachdev, R. Maugi, S. Davis, S.S. Doak, Z. Zhou, M. Platt, Droplet factories: Synthesis and assembly of metal nanoparticles on magnetic supports, J. Colloid Interface Sci. 569 (2020) 204–210. https://doi.org/10.1016/j.jcis.2020.02.087.

[43] R. Moshrefi, A. Suryawanshi, T.J. Stockmann, Electrochemically controlled Au nanoparticle nucleation at a micro liquid/liquid interface using ferrocene as reducing agent, Electrochem. Commun. 122 (2021) 106894. https://doi.org/10.1016/j.elecom.2020.106894.

[44] R. Ishimatsu, F. Shigematsu, T. Hakuto, N. Nishi, T. Kakiuchi, Structure of the Electrical Double Layer on the Aqueous Solution Side of the Polarized Interface between Water and a Room-Temperature Ionic Liquid, Tetrahexylammonium Bis(trifluoromethylsulfonyl)imide, Langmuir. 23 (2007) 925–929. https://doi.org/10.1021/la0623073.

[45] M. Vraneš, A. Tot, S. Jovanović-Šanta, M. Karaman, S. Dožić, K. Tešanović, V. Kojić, S. Gadžurić, Toxicity reduction of imidazolium-based ionic liquids by the oxygenation of the alkyl substituent, RSC Adv. 6 (2016) 96289–96295. https://doi.org/10.1039/c6ra16182k.

[46] E.R. Schreiter, J.E. Stevens, M.F. Ortwerth, R.G. Freeman, A Room-Temperature Molten Salt Prepared from AuCl 3 and 1-Ethyl-3-methylimidazolium Chloride, Inorg. Chem. 38 (1999) 3935–3937. https://doi.org/10.1021/ic990062u.

[47] N. Nishi, A. Suzuki, T. Kakiuchi, Hydrophobic Ionic Liquids Composed of Perfluoroalkyltrifluoroborates for Ionic Liquid–Water Two-Phase Systems, Bull. Chem. Soc. Jpn. 82 (2009) 86–92. https://doi.org/10.1246/bcsj.82.86.

[48] T. Kakiuchi, Ionic-liquid/water: Two-phase systems, Anal. Chem. 79 (2007) 6443–6449. https://doi.org/10.1021/ac0719554.

[49] A. Sabela, V. Mareček, Z. Samec, R. Fuoco, Standard Gibbs energies of transfer of univalent ions from water to 1,2-dichloroethane, Electrochim. Acta. 37 (1992) 231–235. https://doi.org/10.1016/0013-4686(92)85008-9.

[50] G. Taylor, H.H.J. Girault, Ion transfer reactions across a liquid-liquid interface supported on a micropipette tip, J. Electroanal. Chem. 208 (1986) 179–183. https://doi.org/10.1016/0022-0728(86)90307-4.

[51] N. Nishi, S. Imakura, T. Kakiuchi, A digital simulation study of steady-state voltammograms for the ion transfer across the liquid-liquid interface formed at the orifice of a micropipette, J. Electroanal. Chem. 621 (2008) 297–303. https://doi.org/10.1016/j.jelechem.2008.02.004.

[52] H. Hotta, N. Akagi, T. Sugihara, S. Ichikawa, T. Osakai, Electron-conductor separating oil-water (ECSOW) system: A new strategy for characterizing electron-transfer processes at the oil/water interface, Electrochem. Commun. 4 (2002) 472–477. https://doi.org/10.1016/S1388-2481(02)00343-0.

[53] H. Katano, M. Senda, Voltammetry at 1,6-dichlorohexane | Water interface, Anal. Sci. 17 (2001) 1027–1029. https://doi.org/10.2116/analsci.17.1027.

[54] M.H. Abraham, A.F.D. de Namor, Solubility of electrolytes in 1,2-dichloroethane and 1,1-dichloroethane, and derived free energies of transfer, J. Chem. Soc. Faraday Trans. 1 Phys. Chem. Condens. Phases. 72 (1976) 955. https://doi.org/10.1039/f19767200955.

[55] J. Czapkiewicz, B. Czapkiewicz-Tutaj, Relative Scale of Free Energy of Transfer of Anions, J. Chem. Soc. Faraday Trans. 1. 76 (1980) 1663–1668. http://xlink.rsc.org/?DOI=f19807601663.

[56] T. Wandlowski, V. Mareček, Z. Samec, Galvani potential scales for water-nitrobenzene and water-1,2-dichloroethane interfaces, Electrochim. Acta. 35 (1990) 1173–1175. https://doi.org/10.1016/0013-4686(90)80035-M.

[57] A. Uehara, T. Hashimoto, R.A.W. Dryfe, Au electrodeposition at the liquid-liquid interface: Mechanistic aspects, Electrochim. Acta. 118 (2014) 26–32. https://doi.org/10.1016/j.electacta.2013.11.162.

[58] K. Tanaka, N. Nishi, T. Kakiuchi, Electroneutrality Coupling of Electron Transfer at an Electrode Surface and Ion Transfer across the Interface between Thin-layer of 1-Octyl-3-methylimidazolium Bis(perfluoroalkylsulfonyl)imide Covering the Electrode Surface and an Outer Electrolyte Soluti, Anal. Sci. 20 (2004) 1553–1557. https://doi.org/10.2116/analsci.20.1553.

[59] A. Tot, Č. Podlipnik, M. Bešter-Rogač, S. Gadžurić, M. Vraneš, Influence of oxygen functionalization on physico-chemical properties of imidazolium based ionic liquids – Experimental and computational study, Arab. J. Chem. 13 (2020) 1598–1611. https://doi.org/10.1016/j.arabjc.2017.12.011.

[60] J. Wang, Y. Tian, Y. Zhao, K. Zhuo, A volumetric and viscosity study for the mixtures of 1-n-butyl-3-methylimidazolium tetrafluoroborate ionic liquid with acetonitrile, dichloromethane, 2-butanone and N, N ? dimethylformamide, Green Chem. 5 (2003) 618. https://doi.org/10.1039/b303735e.

[61] H. Katano, H. Tatsumi, M. Senda, Ion-transfer voltammetry at 1,6-dichlorohexane|water and 1,4-dichlorobutane|water interfaces, Talanta. 63 (2004) 185–193. https://doi.org/10.1016/j.talanta.2003.10.044.